

Stable tubular microexovesicles of the erythrocyte membrane induced by dimeric amphiphiles

V. Kralj-Iglič*

Institute of Biophysics, Medical Faculty, Lipičeva 2, University of Ljubljana, SI-1000 Ljubljana, Slovenia

A. Iglič

Faculty of Electrical Engineering, Tržaška 25, University of Ljubljana, SI-1000 Ljubljana, Slovenia

H. Hägerstrand

Department of Biology, Åbo Akademi University, Biocity, FIN-20520 Åbo/Turku, Finland

P. Peterlin

Institute of Biophysics, Medical Faculty, Lipičeva 2, University of Ljubljana, SI-1000 Ljubljana, Slovenia

(Received 11 October 1999)

It is experimentally observed that adding a dimeric cationic amphiphile to the erythrocyte suspension results in a release of stable tubular microexovesicles from the erythrocyte membrane. Theoretical description starts from the single-inclusion energy, which takes into account anisotropic shape of the dimeric amphiphile. It is shown explicitly that the tubular shape of the microexovesicle is the extremal to the functional yielding the maximum of the average curvature deviator. It is derived for which intrinsic shapes of the membrane inclusions created by the intercalated amphiphiles the maximum of the average curvature deviator coincides with the minimum of the membrane free energy—thereby determining the stable tubular shape.

PACS number(s): 87.16.Dg, 87.15.Kg

Cell membrane vesiculation, which occurs spontaneously in disordered erythrocytes [1], can be induced in normal erythrocytes by changing the conditions of the erythrocyte suspension. Spontaneous vesiculation of cell membrane is common also in cancer cells [2]. Understanding the mechanisms of shape transformation and vesiculation is important, since it could lead to new methods for manipulating the disordered cells [1].

At sublytic concentrations exogenously added amphiphiles induce changes of the normal discoid shape of erythrocytes into either spiculated echinocytic or invaginated stomatocytic shapes [3]. When incubated with high sublytic concentrations of echinocytogenic amphiphiles the erythrocyte spicules eventually become thinner and shorter while the mother cell becomes spherical [4]. At a certain point,

microexovesiculation occurs [5–7], mostly at the top of the spicules where the skeleton becomes detached from the membrane bilayer. The microexovesiculation starts within some minutes and is completed in about 30 min [6]. The released microexovesicles are so small that they can not be detected under an optical microscope. Analysis of the protein composition of the isolated microexovesicles [7] showed that the microexovesicles are depleted in the membrane skeletal components spectrin and actin, suggesting that a local disruption of the interactions between the membrane skeleton and the membrane bilayer occurred prior to microexovesiculation [5,7,8]. Most species of amphiphiles induce spherical daughter microexovesicles that are formed from sphere-like skeleton free buds [Fig. 1(a)]. However, a cationic dimeric amphiphile N,N' -bisdimethyl-1,2-ethanediamine dichloride derivative



(dioctyl-diQAS) [9] in which two head-tail entities are connected by a spacer at the headgroup level, induces predominantly tubular daughter microexovesicles that are formed from cylindrical buds [Fig. 1(b)]. A certain high sublytic concentration is needed to induce microexovesiculation. The concentration interval where the vesiculation occurs is narrow and close to the concentration that causes hemolysis.

However, the buds on the cell are cylindrical also at lower concentrations than those used to induce the vesiculation. Since the tubular microexovesicles maintained their structure even when isolated prior to fixation this indicates that they are stable for several hours at least.

The currently acknowledged mechanism for description of erythrocyte shape changes is based on the generalized bilayer couple, i.e., area-difference-elasticity model (ADE model) [11] where the equilibrium membrane shape is determined by the minimum of its elastic energy W_{el}

*Electronic address: "vera.kralj-iglic@biofiz.mf.uni-lj.si"

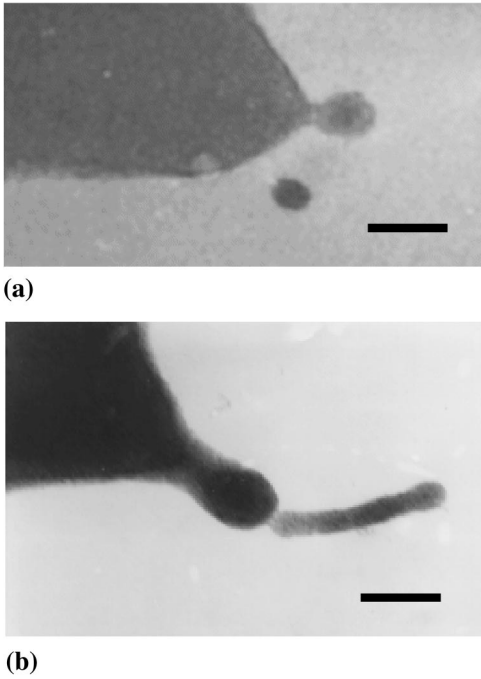


FIG. 1. Transmission electron microscope micrograph of a spherical bud at the top of the echinocyte spicule induced by adding dodecylzwittergent ($263 \mu\text{M}$) to the erythrocyte suspension (a) and of a tubular protrusion at the top of the echinocyte spicule induced by adding dioctyldiQAS ($100 \mu\text{M}$) to the erythrocyte suspension (b). Bars denote 100 nm.

$$W_{el} = \frac{k_c}{2} \int (C_1 + C_2 - C_0)^2 dA + \frac{k_r}{2Ah^2} (\Delta A - \Delta A_0)^2. \quad (1)$$

Here, k_c is the membrane local bending constant, C_1 and C_2 are the principal curvatures describing the local shape of the membrane, C_0 is the spontaneous curvature of the membrane continuum, k_r is the membrane nonlocal bending constant, h is the distance between the two membrane layer neutral areas and ΔA_0 is the area difference of the unstressed layers. The integration is performed over the membrane area A . At large deformations the contribution of the shear energy of the membrane skeleton should also be included [12,13,4].

It was proposed that by intercalating into the membrane the amphiphilic molecules may importantly affect the cell shape, mostly by changing the area difference ΔA_0 . If the molecules intercalate into both membrane layers, ΔA_0 is changed for $(N_{out} - N_{in})a_0$, where N_{out} and N_{in} are the number of the intercalated amphiphilic molecules in the outer and the inner membrane layer, respectively, and a_0 is the area occupied by a single intercalated amphiphilic molecule in the membrane [14].

Fig. 3 shows a sequence of closed axisymmetrical prolate shapes of a given membrane area A and enclosed volume V , and increasing imposed ΔA [14,15]. The shapes were calculated by minimizing the membrane elastic energy [Eq. (1)] for $C_0=0$ and $k_r=\infty$ [15]. A nonzero C_0 and finite k_r do not affect the calculated shape at given ΔA [16]. It can be seen that the shape composed of a cylinder with hemispherical caps corresponds to the minimal possible ΔA while the

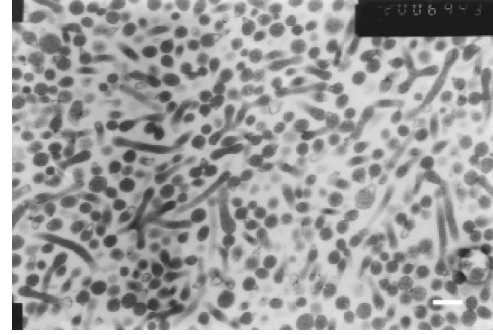


FIG. 2. Transmission electron microscope micrograph of the isolated tubular daughter microexovesicles induced by adding dioctyldiQAS to the erythrocyte suspension. The method for preparing the microexovesicles for observation is described in Ref. [10]. The microexovesicles in the sample were oriented randomly. The white bar denotes 100 nm.

shape composed of spheres corresponds to the maximal possible ΔA within the given class of shapes.

In our experiments the erythrocytes first underwent a discocyte-echinocyte transformation [4] and proceeded to develop exovesicles, so it is evident that within the given class of shapes the area difference ΔA continuously increased in the process. At the present state of the development of the theoretical models we cannot describe the whole process of the transformation of the erythrocyte from the discocyte to the state of microexovesiculation. We can however study the final shape of the microexovesicles. Fig. 3 shows that at given relative volume the spherical microexovesicles yield a higher ΔA than the tubular ones. Moreover, the tubular microexovesicles give the lowest possible ΔA within this class. According to the bilayer couple model the process of increasing the area difference of the unstressed membrane layers ΔA_0 would increase the equilibrium ΔA , leading to spherical daughter microexovesicles. However, the tubular character of the daughter microexovesicles that is evident already from the shape of the bud [Fig. 1(b)] persists

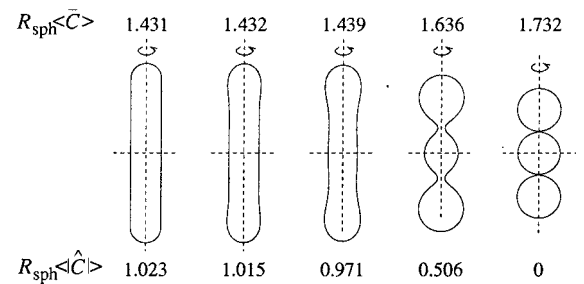


FIG. 3. A sequence of axisymmetric vesicle shapes of the area A and the volume V given by the relative volume $v = \sqrt{36\pi V^2/A^3} = 1/3^{1/2}$. The sequence was obtained by increasing an imposed relative difference between the outer and the inner membrane layer areas $\Delta A/8\pi R_{\text{sph}}$, i.e., the relative average mean curvature $R_{\text{sph}} \langle \bar{C} \rangle$. Here R_{sph} is the radius of the sphere of the area A , $R_{\text{sph}} = (A/4\pi)^{1/2}$. The corresponding values of the relative average mean curvature and the relative average curvature deviator $R_{\text{sph}} \langle \hat{C} \rangle$ are given. All the shapes but the first one were calculated by minimizing the membrane elastic energy [Eq. (1)] (Ref. [15]). The first shape was obtained by combining the solutions of Eq. (8) representing the sphere and the cylinder.

also when the vesicles are pinched off from the membrane (Fig. 2), although their area difference could be further increased by yielding spherical microexovesicles. It is therefore concluded that the ADE model in its present form cannot give an explanation for the stable tubular microexovesicle shape. These conclusions are supported by the recent theoretical results [17], which claim that stable tubular structures of the membrane can not be explained by the ADE model.

In order to explain the observed tubular shape of the erythrocyte daughter microexovesicles we upgrade the ADE model [11] by taking into account the specific shape of the dimeric amphiphile dioctyldiQAS. In the dioctyldiQAS molecule the two head-tail entities are joined by a spacer in the headgroup level thereby forming an anisotropic molecule. We assume that intercalated anisotropic amphiphiles in the membrane create anisotropic inclusions that can orient in the curvature field of the membrane [18–20].

We pursue the basic mechanism deriving from the coupling between the orientation of the anisotropic inclusion and the difference between the two principal membrane curvatures [18]. Due to this coupling the anisotropic inclusions undergo orientational ordering in the regions where the difference between the two principal curvatures is large enough (e.g., in thin tubular protrusions and in narrow necks) thereby stabilizing the shape with thin tubular protrusions and/or narrow necks [20].

The orientation of the inclusion is given by the rotation of the principal directions of the intrinsic shape relative to the membrane principal directions ω . The single-inclusion energy derives from the mismatch between the local membrane shape and the intrinsic shape of the inclusion [19,20],

$$E(\omega) = \frac{\xi}{2}(\bar{C} - \bar{C}_m)^2 + \frac{1}{2} \frac{\xi + \xi^*}{2} [\hat{C}^2 - 2\hat{C}\hat{C}_m \cos(2\omega) + \hat{C}_m^2], \quad (2)$$

where ξ and ξ^* are positive interaction constants, $\bar{C} = \frac{1}{2}(C_1 + C_2)$, $\hat{C} = \frac{1}{2}(C_1 - C_2)$, $\bar{C}_m = \frac{1}{2}(C_{1m} + C_{2m})$, $\hat{C}_m = \frac{1}{2}(C_{1m} - C_{2m})$, and C_{1m} and C_{2m} are the principal curvatures describing the intrinsic shape of the inclusion. If $\hat{C}_m = 0$ the inclusion is isotropic while if $\hat{C}_m \neq 0$ the inclusion is anisotropic.

It was found [21] that dimeric amphiphilic molecules in which the headgroups are joined by a C_sH_{2s} , ($s = 1, 2, 3 \dots$) spacer form cylindrical micelles in water when the spacer is short (low s values). In the dioctyldiQAS molecule $s = 2$, therefore we assume that at least one of the intrinsic principal curvatures of the inclusion is much larger than any curvature on the erythrocyte membrane. Consequently, $|\hat{C}_m|$ is much larger than any $|\bar{C}|$ or $|\hat{C}|$ on the membrane. The intrinsic average curvature $|\bar{C}_m|$ may also be large. Therefore, we retain in the single-inclusion energy only the terms proportional to \bar{C}_m and \hat{C}_m ,

$$E(\omega) = -\xi\bar{C}\bar{C}_m - \frac{\xi + \xi^*}{2} \hat{C}\hat{C}_m \cos(2\omega), \quad (3)$$

where we disregarded the constant contributions.

To account for the different orientational states the partition function of a single inclusion is introduced [18,20], $q = 1/2\pi \int_0^{2\pi} \exp[-E(\omega)/kT] d\omega$, where k is the Boltzmann constant, T is the temperature and $E(\omega)$ is given by Eq. (3). The corresponding free energy of the single inclusion $F_i = -kT \ln q$ is

$$F_i = -\xi\bar{C}_m\bar{C} - kT \ln \left[I_0 \left(\frac{\xi + \xi^*}{2kT} \hat{C}_m \hat{C} \right) \right], \quad (4)$$

where the integration over ω yielded the modified Bessel function I_0 [18]. For $(\xi + \xi^*)|\hat{C}||\hat{C}_m|/2kT \gg 1$ [20], the single-inclusion free energy is up to a constant equal to

$$F_i = -\xi\bar{C}_m\bar{C} - \frac{1}{2}(\xi + \xi^*)|\hat{C}||\hat{C}_m|. \quad (5)$$

The absolute value of \hat{C} is called the curvature deviator [22].

We limit the study to the analysis of the shape of the daughter microexovesicles (Figs. 2 and 3). We found that the membrane skeleton is not present in shed microexovesicles. Therefore we need not consider the shear energy of the membrane skeleton. The free energy of the membrane F is the sum of the two contributions: the membrane elastic energy and the energy of the interaction between the inclusions and the membrane continuum.

Considering the above arguments regarding the much larger intrinsic curvature of dioctyldiQAS-induced inclusions than any curvature attained by the membrane, we can neglect all the terms in Eq. (1) aside possibly from the contribution due to the intercalated dioctyldiQAS, to the area difference ΔA_0 , $(N_{out} - N_{in})a_0$ [23]. Also, it is assumed that the membrane is very thin so that $\Delta A = 2h\int \bar{C} dA$. Therefore, the membrane elastic energy is up to a constant given by an approximate expression $W_{el} \approx -(k_r/Ah^2)\Delta A\Delta A_0 = -(2k_r a_0/Ah)(N_{out} - N_{in})\int \bar{C} dA$. The energy of the interaction between the inclusions and the membrane continuum F_m is obtained by multiplying the free energy of a single inclusion [Eq. (5)] by the area density of the inclusions and integrating over the corresponding layer area. The contributions of both layers are added up, $F_m = \int n_{out} F_i(C_1, C_2) dA + \int n_{in} F_i(-C_1, -C_2) dA$. We assume for simplicity that the inclusions are distributed homogeneously over the membrane layer area so that the respective area densities are $n_{out} = N_{out}/A$ and $n_{in} = N_{in}/A$. The membrane free energy F is

$$F = -\alpha\langle\bar{C}\rangle - \beta\langle|\hat{C}|\rangle, \quad \alpha \neq \beta, \quad (6)$$

where $\alpha = (n_{out} - n_{in})A(\xi\bar{C}_m + 2k_r a_0/h)$, $\beta = \frac{1}{2}(n_{out} + n_{in})A(\xi + \xi^*)|\hat{C}_m|$, the average mean curvature is $\langle\bar{C}\rangle = (1/A)\int \bar{C} dA$ and the average curvature deviator is $\langle|\hat{C}|\rangle = (1/A)\int |\hat{C}| dA$. The parameter β is always positive, while for echinocytogenic amphiphiles α is also positive.

The instantaneous equilibrium shape is determined by the minimum of the membrane free energy. To find the minimum of the membrane free energy F [Eq. (6)] at a given area of the membrane A , and a given volume enclosed by the membrane V , we construct a functional G

$$G = F - \lambda_A \left(\int dA - A \right) - \lambda_V \left(\int dV - V \right), \quad (7)$$

where λ_A and λ_V are the Lagrange multipliers, and dV is the volume element. The symmetry axis of the body has been chosen to coincide with the x axis, so that the shape is given by the rotation of the function $y(x)$ around the x axis. In this case the principal curvatures are expressed by $y(x)$ and its derivatives with respect to x ; $y' = \partial y / \partial x$ and $y'' = \partial^2 y / \partial x^2$, as $C_1 = 1/y\sqrt{1+y'^2}$ and $C_2 = -y''/(1+y'^2)^{3/2}$. The area element is $dA = 2\pi\sqrt{1+y'^2}y dx$, and the volume element is $dV = \pi y^2 dx$. The sign of the principal curvatures is taken to be positive for a sphere. We take into account that C_1 is always larger than C_2 for the elongated shapes with high anisotropy. The above variational problem can be expressed by the Euler-Poisson equation [24]. By using the expressions for C_1 , C_2 , dA and dV the Euler-Poisson equation attains the form

$$\frac{2y''}{(1+y'^2)^2} + \lambda_A \left[\frac{1}{\sqrt{1+y'^2}} - \frac{yy''}{(\sqrt{1+y'^2})^3} \right] - y\lambda_V = 0, \quad (8)$$

where $-\lambda_A/2\pi(\alpha-\beta) \rightarrow \lambda_A$, $\lambda_V/2\pi(\alpha-\beta) \rightarrow \lambda_V$. The solution of Eq. (8) given by the ansatz $y = \lambda_A/\lambda_V$ represents a cylinder of the radius $r_{\text{cyl}} = \lambda_A/\lambda_V$ while another solution given by a circle of the radius r_{cir} and the origin $(x_0, 0)$, $y = \sqrt{r_{\text{cir}}^2 - (x-x_0)^2}$, fulfills Eq. (8) for two different radii, $1/r_{\text{cir},1,2} = (\lambda_A \pm \sqrt{\lambda_A^2 - 2\lambda_V})/2$. By combining the above solutions it can be shown that the cylinder closed by two hemispheres fulfills the conditions for the extreme [24] when the two Lagrange multipliers are interdependent $\lambda_A^2 = 2\lambda_V$, while $r_{\text{cyl}} = r_{\text{cir}}$.

In this work we introduce the average curvature deviator $\langle |\hat{C}| \rangle_{\text{max}}$ as a parameter that is important in determination of the vesicle shape. Figure 3 shows that the shape composed of the cylinder and two hemispheres corresponds to the maximal average curvature deviator $\langle |\hat{C}| \rangle_{\text{max}}$ and the minimal average mean curvature $\langle \bar{C} \rangle_{\text{min}}$. The shape composed of three spheres corresponds to the maximal average mean curvature

$\langle \bar{C} \rangle_{\text{max}}$ [16,25,15] while its average curvature deviator is 0 and therefore minimal. It follows from Eq. (6) that the tubular shape corresponds to the minimum of the membrane free energy if

$$\beta > \alpha (\langle \bar{C} \rangle_{\text{max}} - \langle \bar{C} \rangle_{\text{min}}) / \langle |\hat{C}| \rangle_{\text{max}}, \quad (9)$$

else the shape of the minimal membrane free energy is composed of spheres. The tubular shape would be favored best by anisotropic molecules that intercalate into both membrane layers while the spherical shape would be favored best by isotropic molecules that intercalate into one membrane layer.

To conclude, our results indicate that the deviatoric properties of the membrane induced by orientational ordering of the anisotropic inclusions are a possible plausible explanation for the observed stable tubular shape of the microexovesicles released from erythrocyte membrane upon incubation with dimeric amphiphiles at high sublytic concentrations.

The deviatoric properties of the membrane were also suggested to explain the experimentally observed tubular structures in the geraniol-dimyristoylphosphatidylcholine-water system [26] that could not be explained by the ADE model.

For smoothly and slowly varying curvatures of the thin membrane, the bilayer part of the membrane can be well described as a two-dimensional liquid. However, whenever the membrane due to some reason develops regions of large difference between the two principal curvatures, the anisotropic membrane constituents orient in these regions. We can say that the membrane there exhibits properties of a two-dimensional liquid crystal which importantly influence the cell shape.

Another effect that may play an important complementary role in development of the tubular protrusions and microexovesicles is a nonuniform lateral distribution of the membrane constituents [27,19,20].

Considering other mechanisms that may be relevant in the physics of tubular structures it should be noted that thin tubular structures of surfactant molecules were observed also in shear flow without the presence of the dimeric amphiphiles [28].

-
- [1] J. Palek, *Blood Rev.* **1**, 147 (1987); G. M. Wagner, D. T. Y. Chiu, M. C. Yee, and B. H. Lubin, *J. Lab. Clin. Med.* **108**, 315 (1986).
- [2] R. A. Black *et al.*, *Nature (London)* **385**, 729 (1997).
- [3] B. Deuticke, *Biochim. Biophys. Acta* **163**, 494 (1968).
- [4] A. Iglić, V. Kralj-Iglić, and H. Hägerstrand, *Eur. Biophys. J.* **27**, 335 (1998).
- [5] S. C. Liu, L. H. Derick, M. A. Duquette, and J. Palek, *Eur. J. Cell Biol.* **49**, 358 (1989).
- [6] H. Hägerstrand and B. Isomaa, *Biochim. Biophys. Acta* **1109**, 117 (1992).
- [7] H. Hägerstrand and B. Isomaa, *Biochim. Biophys. Acta* **1190**, 409 (1994).
- [8] A. Iglić, S. Svetina, and B. Žekš, *Biophys. J.* **69**, 274 (1995); A. Iglić and H. Hägerstrand, *Med. Biol. Eng. Comput.* **37**, 125 (1999).
- [9] B. Rozycka-Roszak, S. Witek, and S. Przystalski, *J. Colloid Interface Sci.* **131**, 181 (1989).
- [10] H. Hägerstrand and B. Isomaa, *Biochim. Biophys. Acta* **982**, 179 (1989).
- [11] E. Evans, *Biophys. J.* **14**, 923 (1974); W. Helfrich, *Z. Naturforsch. C* **29**, 510 (1974); W. Wiese, W. Harbich, and W. Helfrich, *J. Phys.: Condens. Matter* **4**, 1647 (1992); V. Heinrich, S. Svetina, and B. Žekš, *Phys. Rev. E* **48**, 3112 (1993); L. Miao, U. Seifert, M. Wortis, and H. G. Döbereiner, *ibid.* **49**, 5389 (1994).
- [12] E. Sackmann, *FEBS Lett.* **346**, 3 (1994).
- [13] R. E. Waugh, *Biophys. J.* **70**, 1027 (1996).
- [14] L. Miao, B. Fourcade, M. Rao, M. Wortis, and R. K. P. Zia, *Phys. Rev. A* **43**, 6843 (1991); U. Seifert, *Adv. Phys.* **46**, 13 (1997).
- [15] A. Iglić, V. Kralj-Iglić, and J. Majhenc, *J. Biomech.* **32**, 1343 (1999).
- [16] S. Svetina and B. Žekš, in *Handbook of Nonmedical Application of Liposomes*, edited by D. D. Lasic and Y. Barenholz,

- (CRC Press, Boca Raton, 1996), p. 13.
- [17] J.-B. Fournier and P. Galatola, *Europhys. Lett.* **39**, 225 (1997).
- [18] J.-B. Fournier, *Phys. Rev. Lett.* **76**, 4436 (1996).
- [19] V. Kralj-Iglič, S. Svetina, and B. Žekš, *Eur. Biophys. J.* **24**, 311 (1996).
- [20] V. Kralj-Iglič, V. Heinrich, S. Svetina, and B. Žekš, *Eur. Phys. J. B* **10**, 5 (1999).
- [21] R. Zana and Y. Talmon, *Nature (London)* **362**, 228 (1993); R. Oda, I. Huc, and S. J. Candau, *Chem. Commun. (Cambridge)*, 2105 (1997).
- [22] T. M. Fischer, *J. Phys. II* **3**, 1795 (1992).
- [23] We do not have direct experimental evidence about the preference of the dioctyldiQAS molecule for either of the membrane layers, however it was suggested (Refs. [6] and [13]) that echinocytogenic amphiphiles intercalate preferentially into the outer membrane layer.
- [24] L. E. Elsgolc, *Calculus of Variations*, (Pergamon Press, Oxford, 1961).
- [25] A. Iglič, H. Hägerstrand, V. Kralj-Iglič, and M. Bobrowska-Hägerstrand, *J. Biomech.* **31**, 151 (1998).
- [26] C. R. Safinya, *Colloids Surf. A* **128**, 183 (1997).
- [27] D. Andelman, T. Kawakatsu, and K. Kawasaki, *Europhys. Lett.* **19**, 57 (1992); F. Jülicher, and R. Lipowsky, *Phys. Rev. Lett.* **70**, 2964 (1993); A. A. Boulbitch, *Phys. Rev. E* **56**, 3395 (1997); P. G. Dommersnes and J.-B. Fournier, *Eur. Phys. J. B* **12**, 9 (1999).
- [28] E. Mendes, J. Narayanan, R. Oda, F. Kern, S. J. Candau, and C. Manohar, *J. Phys. Chem. B* **101**, 2256 (1998); E. Mendes, R. Oda, C. Manohar, and J. Narayanan, *ibid.* **102**, 338 (1998); N. Shahidzadeh, D. Bonn, O. Aguerre-Chariol, and J. Meunier, *Phys. Rev. Lett.* **81**, 4268 (1998).